Journal of Catalysis 269 (2010) 64–70

Contents lists available at ScienceDirect

Journal of Catalysis

journal homepage: www.elsevier.com/locate/jcat

Further investigations on Constraint Index testing of zeolites that contain cages

John R. Carpenter [a], Sheila Yeh [b], Stacey I. Zones [b], Mark E. Davis [a,*]

[a] Chemical Engineering, California Institute of Technology, Pasadena, CA 91125, USA
[b] Chevron Energy Technology Company, 100 Chevron Way, Richmond, CA 94802, USA

ARTICLE INFO

Article history:
Received 6 August 2009
Revised 8 October 2009
Accepted 19 October 2009
Available online 22 November 2009

Keywords:
Constraint Index test
Zeolite shape selectivity
Cage effect
Hexane cracking
Structure–selectivity relationship
External surface dealumination

ABSTRACT

Zeolites such as SSZ-25 and SSZ-35 exhibit Constraint Indexes (CI) lower than expected. Two hypotheses for the origin of the lower CI values are that partial cages on the external surface of the zeolites significantly contribute to the overall conversions and that the large cages within the crystalline structures provide less steric hinderence at the active site than would be expected from the size of the pores. The effect of external surface activity is observed by comparing the as-synthesized materials to those passivated via dealumination with ammonium hexafluorosilicate. The external surface dealumination is verified by XPS and by the reduction in reactivity toward isopropanol dehydration observed from materials still containing their SDAs. The external surface of calcined zeolites is shown to have little influence on the CI value. Cage accessibility is investigated by comparisons of structures having larger cages to those that do not and by following the time dependent behavior of the CI values for these materials. The presence of large cages in the zeolites is shown to lower the CI values below those expected from the pore sizes, and the time dependence of the CI value can provide insight into the existence of these larger cage structures.

1. Introduction

As the library of zeolite and zeolitic materials has expanded over the years, many techniques to determine both structure and shape selectivity of these materials have been developed. One of the reaction tests first described was the Constraint Index (CI) that is based on the competitive cracking of 3-methylpentane and *n*-hexane [1]. The CI is calculated by Eq. (1) (*X* denotes the fractional conversion of each species) and thus it is proportional to the observed cracking rate constants of *n*-hexane to 3-methylpentane.

$$\mathrm{CI} = \frac{\log(1 - X_{n\text{-hexane}})}{\log(1 - X_{3\text{-methylpentane}})} \quad (1)$$

In describing the CI test, Frillette and colleagues detailed a test method to classify zeolites on the basis of their shape selective properties that can provide insight into the structure of the zeolite. Specifically the goal of the CI test was to easily identify zeolites with properties and structures similar to ZSM-5 [1]. From Eq. (1), it can be seen that the more selective a material is for cracking *n*-hexane the higher the CI value for that material will be. On the basis of CI value, Frillette et al. classified materials with a CI value greater than 12 as small pores (that is, having 8-ring pores or less); CI values less than 1 defined as large pores (12-ring pores or greater), and materials with CI values between 1 and 12 intermediate pores (10-ring pores) [1]. Table 1 lists examples of various zeolites and their CI values [2].

While the CI test classifies zeolites on the basis of pore size, Frillette et al. in detailing the method also discuss the influence of the internal void space of the structure on the test [1]. The notion of shape selectivity resulting from the internal void space is a well-known notion termed by Csicsery as restricted transition-state selectivity [3]. While at the time of Frillette et al.'s description of the CI test, pore size sufficiently ranked the known materials that typically consisted of tubular pores. Later advances in materials leading to even more complex structures has advanced the idea of probing the internal void space as has been noted for example in a review by Jacobs and Martens [4]. Some ambiguity can also arise from the fact that the term "pore" can have multiple meanings referring to either the portal to the interior of the structure or to the entire passage space through the structure. In this study the use of "pore" refers to the ring opening that acts as a portal into the structure.

In a previous study Zones and Harris detailed several examples of zeolites with known portal sizes that have CI results inconsistent with these sizes [2]. For example, SSZ-35 gave a CI value below 1 and a cracking rate of the larger 3-methylpentane higher than that of *n*-hexane in the test, even though the portal for the structure is 5.5 Å [5] which is not much larger than that of ZSM-5. For a number of the materials in the Zones/Harris study, where there were deviations from expectations, it appeared that the structures, once known, had portals that opened into larger cages.

* Corresponding author. Fax: +1 626 568 8743.
E-mail address: mdavis@cheme.caltech.edu (M.E. Davis).

0021-9517/$ - see front matter © 2009 Elsevier Inc. All rights reserved.
doi:10.1016/j.jcat.2009.10.016

Table 1
Examples of reported CI values for various structures [2].

Zeolite	Pore apertures	CI
SSZ-13	8-Ring	>100
Erionite	8-Ring	38
ZSM-23	10-Ring	10.6
SSZ-20	10-Ring	6.9
ZSM-5	10- & 10-Rings	6.9
EU-1	10-Ring	3.7
ZSM-12	12-Ring	2.1
SSZ-31	12-Ring	0.9
LZY-82	12-Ring	0.4
CIT-5	14-Ring	0.4
SSZ-24	12-Ring	0.3
UTD-1	14-Ring	0.3
SSZ-25	10- & 10-Rings	0.8
SSZ-35	10-Ring	0.6

It is important to note that since the introduction of the CI test much research has gone into the development of other catalytic tests for zeolite characterization ranging from the characterization of large pore zeolites to comparing acid site strength to probing void spaces. A few of these, but not meant to be a complete list, are tests on acid zeolites like the Shape Selectivity Index with *m*-xylene isomerisation [6], the alkylation of *meta*-diisopropylbenzene [7], the conversion of methanol to larger hydrocarbons [8] and bifunctional catalyst tests such as the Modified Constraint Index [9] and the Spaciousness Index [10]. Both Ribeiro et al. [11] and Jacobs and Martens [4] describe these and several other valuable catalytic tests for zeolite characterization in reviews of the structure–activity relationship in zeolites, covering both acid and bifunctional catalyses. This study focuses on the CI test's cracking reaction as it is still used as a key characterization method in many patents for new materials. It is also quick and convenient to operating at atmospheric pressure. The CI test has been employed to help determine the structures of new materials such as IM-5 and SSZ-57 [12].

In this study, we focus on two materials, SSZ-25 and SSZ-35. In SSZ-35 there are 10-ring portals that connect large 18-ring cages. Likewise SSZ-25, once calcined, has 12-ring cages that are accessed by 10-ring portals. Fig. 1 depicts the structures of SSZ-25 and SSZ-35 with their 10-ring pores opening into larger cages and the materials we use here for comparison, namely ZSM-5 and zeolite beta (denoted here as BEA). Fig. 2 shows the two different structure directing agents (SDAs) used in synthesizing the cage containing zeolites SSZ-25 and SSZ-35. Here, we address two hypotheses for the origin of the lower CI values in SSZ-25 and SSZ-35 that are:

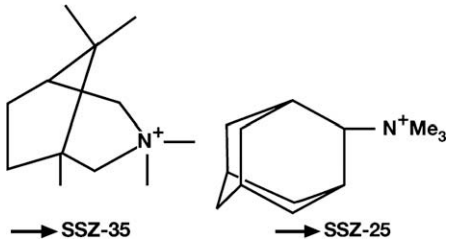

Fig. 2. Structure-directing agents (SDAs) for the caged structures SSZ-25 and SSZ-35.

(i) partial cages on the external surface of the zeolites significantly contribute to the overall conversions, and (ii) the large cages within the crystalline structures provide less steric hinderence at the active site than would be expected from the size of the pores.

2. Experimental

2.1. Zeolite synthesis and procurement

The zeolites used in the study were synthesized in all cases except for zeolites BEA and mordenite (MOR). BEA was obtained from the TOSOH Corporation as product number HSZ930NHA (still contains the SDA). Unless specified, the BEA sample was calcined and 2 ion-exchanges with ammonium nitrate (95 °C, 2 h) were performed before use. Mordenite was obtained from Zeolyst with a Si/Al of 6.5 and as with the BEA it underwent 2 ion-exchanges with ammonium nitrate. Samples of the NH_4-MOR (~2 g) were partially exchanged using the conditions in previous work by Iglesia and coworkers [13] with 70 mL of a 2.4 M aqueous $NaNO_3$ solution for 12 h at 80 °C then washed with excess deionized water. Both the parent and partially exchanged mordenite samples were calcined at 550 °C before use.

2.1.1. ZSM-5

In a 23 mL Teflon Cup for a Parr 4845 reactor the following reagents were combined. 0.11 g of Reheis F-2000 alumina hydroxide gel (25% Al) was dissolved into a basic solution of 1.9 g of 40% tetrapropylammonium hydroxide, 3.35 g of 1 N NaOH, and 1 mL water. Once the solution was clear, 4.5 g of Ludox AS-30 was added with stirring. The reactor was closed, loaded onto a spit in a convection heated oven and tumbled while being heated at 170 °C for 5 days. The product was collected upon cooling and verified to be ZSM-5 by XRD analysis. The product was then calcined to

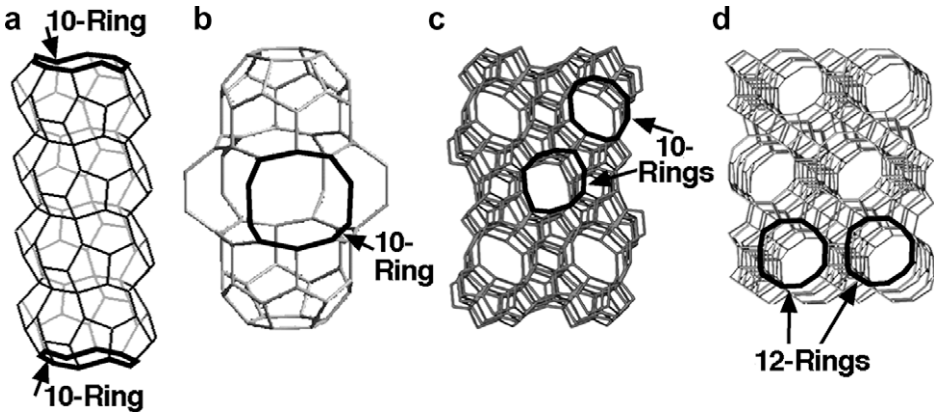

Fig. 1. Structures of zeolites discussed in this paper highlighting pore openings into the various cage and channels: (a) SSZ-35 (**STF**), (b) SSZ-25 (**MWW**), (c) ZSM-5 (**MFI**) and (d) BEA (*__BEA__).

595 °C by a program of heating at 1 °C/min to 120 °C (hold for 2 h), at 1 °C/min to 540 °C (hold for 5 h), and at 1 °C/min to 595 °C (hold for 5 h) to remove the SDA. After which, 2 ion-exchanges with ammonium nitrate solution (95 °C, 2 h each) were performed before use in catalytic studies.

2.1.2. SSZ-25

The sample of SSZ-25 used in this study was taken from a 5 gallon preparation of the material using a mixed SDA system of *N*,*N*,*N*,2-trimethyladamantammonium hydroxide (see Fig. 2) and piperidine as a pore filler [14]. A similar post-crystallization treatment schedule as with ZSM-5 was provided except the SSZ-25 was given 4 ion-exchanges treatments after the calcination.

2.1.3. SSZ-35

The sample of SSZ-35 was taken from a batch made in a 1 gallon reactor run at 160 °C, 75 RPM for a course of 16 days. The ratio of reagents was as follows: the organo-cation to SiO_2 ratio was 0.10 with the reagents being the SDA from pentamethyl (1,6,6,8,8) bicyclo[3.2.1]-6-ammonium-octane (Fig. 2) and Ludox AS-30 (30% SIO_2). SiO_2/Al_2O_3 = 35 with Reheis F-2000 as an Al source. KOH/SiO_2 = 0.20 and H_2O/SiO_2 = 35.

2.2. External surface modification

The external surfaces of the zeolites were dealuminated following the procedure described by Breck and Skeels [15] using an aqueous ammonium hexafluorosilicate treatment. Samples were used before calcinations to maintain the SDA inside the structure. Two grams of zeolite were stirred in 50 mL of an aqueous ammonium acetate solution (2 M, 75 °C). Separately, 1.5 g ammonium hexafluorosilicate was dissolved in 50 mL of water. The ammonium hexafluorosilicate solution was added dropwise over 3 h to zeolite mixture once the mixture had reached 75 °C. After the addition of the ammonium hexafluorosilicate solution was complete, the mixture was heated to 95 °C and stirred with condenser for 12 h. The zeolite was then filtered from the mixture and washed with a minimum of 500 mL hot water before air drying.

2.3. Reactions

Zeolite samples were tested using the CI test reaction and the isopropanol dehydration reaction by pelletizing and then crushing the pellet of either the acid or NH_4^+-form of the zeolites. The sample was sieved to collect the 20–40 mesh fraction. Typically 0.50 g (~1 mL) of sample was loaded into the reactor tube packed between glass wool. The sample was then heated to 350 °C under an argon flow of 25 cm^3/min for at least 4 h before reactions commenced.

Reactions were carried out in a BTRS Jr. single pass vertical reactor system (Autoclave Engineers) using a stainless steel reactor tube. The hydrocarbon feed was fed as a liquid with a syringe pump into a mixing assembly where it was vaporized with a sweep gas of 5% argon in helium (AirLiquide, 99.999%) in a mixing assembly at 150 °C. Products were analyzed by online GC/MS (Agilent GC 6890/MSD 5973N) with a Plot-Q capillary column.

Conditions for a typical Constraint Index test or single reactant cracking reaction were a reaction temperature of 330 °C and atmospheric pressure with 0.5 g of zeolite. The reactant liquid feed was at a LHSV of 1.67 h^{-1}. Isopropanol dehydration used a lower temperature of 150 °C. *n*-Hexane, 3-methylpentane, and isopropanol were all used as purchased from Aldrich with purities greater than 99.9%. For the Constraint Index test a mixture of 50 mol% *n*-hexane and 50 mol% 3-methylpentane was used.

2.4. Zeolite characterization

Zeolite structures were determined by powder X-ray diffraction using a Scintag XDS 2000 diffractometer. Micropore volumes of the zeolites were measured by nitrogen adsorption on a Micromeritics ASAP 2000 instrument. SEM images were obtained from a LEO 1550 VP field emission scanning electron microscope, and the images were used to measure crystal sizes. Elemental analysis data for calculating the silicon to aluminum ratio (SAR) of the bulk material were obtained from Galbraith Analytical in Knoxville, TN. Thermogravimetric analyses were done with a NETZSH STA 449C analyzer and the results utilized for measuring the temperature where the SDA was lost (from as-synthesized samples) and carbonaceous residue content for samples after reaction. The temperature was increased at the rate of 5 °C/min with air used as a sweep gas. The measurements of surface compositions were made using a commercial XPS, an Ulvac Phi Quantera Scanning Microprobe. The particles making up the samples were small grain and closely packed for analysis. The X-ray spot defining the analysis area was a rectangle 1.4 mm × 0.1 mm, so many analyses sampled multiple particles. The scans were made with a nominal spectral resolution of 1.05 eV. For all samples multiple analysis areas were scanned, and the tabulated data represent the determined average and standard deviation. The XPS raw signal intensities were normalized using empirical sensitivity factors by standard XPS data handling software, and compositions are given in atom%.

3. Results and discussion

3.1. Contributions of the external surface to the CI values

The external surfaces of SSZ-25, SSZ-35, ZSM-5, and BEA were dealuminated to minimize the contribution of the external surface to their respective CI values. Table 2 details the characterizations of each sample for both the parent zeolites and their dealuminated versions (D – denotes dealuminated samples). Each sample was dealuminated following the process of Breck and Skeels [15] with the exception of performing the treatment on as-synthesized samples. This was done in order to maintain the SDA in the zeolite during the treatment to block the dealuminating agent from the interior of the zeolite and thus limit the dealumination to the external surface. XPS analysis demonstrates a larger increase in the superficial Si/Al ratio than the change in the bulk Si/Al measured by elemental analysis for each zeolite. It should be noted that the XPS technique samples deeper than just the external surface of the zeolite and thus the actual Si/Al ratio for the external surface may be higher than that given by the XPS measurement. XRD and SEM analyses show little change in the crystallinity and crystal

Table 2
Zeolites properties before and after surface modification.

Zeolite	Surface Si/Al[a]	Bulk Si/Al[b]	Micropore volume (cc/g)[c]	Isopropanol reaction rate (μmol/min/g)
BEA*	16.6	13.5	0.22	18
D-BEA*[d]	21.4	19.7	0.18	2
ZSM-5	21.5	19.4	0.13	1.1
D-ZSM-5[d]	72.6	19.8	0.11	0.5
SSZ-25	18.2	16.0	0.13	NA
D-SSZ-25[d]	40.9	23.6	0.11	NA
SSZ-35	17.9	16.3	0.15	1.8
D-SSZ-35[d]	26.4	20.2	0.11	0.6

[a] Surface Si/Al determined by XPS.
[b] Bulk Si/Al determined by ICP.
[c] Determined by *t*-plot method.
[d] D – denotes dealuminated samples.

size, respectively, of each sample after the treatment (all four zeolite samples used in this study had crystal sizes of 0.5 μm or less).

Isopropanol dehydration was used to characterize the effect of the dealumination process on the BEA, ZSM-5, and SSZ-35 samples as a low temperature reaction, 150 °C, since the SDA remains in the structure to block access to the internal pore space. The zeolites were activated by a thermal pretreatment in a flowing stream of inert gas. 350 °C was found to be the lowest pretreatment temperature that could be used for activation to achieve the full activity of each material tested. This temperature is low enough to maintain the SDA in the structures of ZSM-5, BEA, and SSZ-35. However, for SSZ-25, its SDA undergoes decomposition at temperatures below 350 °C, and thus it cannot be characterized in this manner. There was no increase in the porosity of the ZSM-5, BEA, or SSZ-35 samples containing SDA after use in the isopropanol reaction. Table 2 lists the reaction rate of isopropanol decomposition at 15 min on stream and at 150 °C. The dealumination process did not completely eliminate the activity of the samples. However, for all three samples tested, the reduction in the isopropanol reaction rate is greater than 50%.

Fig. 3 shows the comparison of the CI tests for calcined samples of the parent and dealuminated zeolites. The observed behavior of BEA and ZSM-5 is as expected for these structures based on the published literature. BEA has a high initial activity that is followed by quick deactivation with a CI value of 0.8, while ZSM-5 has a CI value between 7 and 8 with little deactivation over the 6 h on stream. The dealumination process appears to only slightly reduce the activity for both zeolites with no effect on the CI values. The reduced activity is attributed to the loss of pore volume during the dealumination treatment. Similarly SSZ-35 also shows only a small reduction in activity and similar CI values over time online between the parent sample and the surface dealuminated sample. For all three samples, the external surface has little impact on the CI value, and thus cannot be the reason for the low CI value of SSZ-35. Further evidence for the lack of external surface contribution can be observed using an SSZ-35 that still contains the SDA that can serve as a pore blocking agent. For SSZ-35, the SDA remains intact even at the conditions of the CI test. When the CI test is run on SSZ-35 that contains the SDA, no cracking is observed.

Unlike the other zeolites tested, SSZ-25 does show differences between the behavior of the parent and dealuminated sample in the CI test. The initial 45 min of time online are similar. However, later, the dealuminated sample deactivates quicker than the parent sample and the CI value of the dealuminated sample increases at a slower rate. This change in the CI value is opposite to that expected if open cages on the external surface were making a significant contribution to the cracking reaction. The external surface might be expected to have no shape selectivity and thus lower the CI value. Reducing the external surface effect by dealumination would be expected to give a higher initial CI value. As such, the external surface does not appear to be responsible for the low CI value of SSZ-25.

The CI test behavior of SSZ-25 observed here is consistent with a recent study on the transformation of *n*-heptane over MCM-22. In that work, the authors suggested that the large initial drop in activity is from the deactivation of the large cages by coke formation with a quasi-plateau in activity remaining from the smaller sinusoidal pores [16]. The activity pattern shown in Fig. 4d for SSZ-25 follows the same deactivation behavior for the CI test as was observed with the *n*-heptane cracking on MCM-22. The increasing CI value over time on stream may then be a consequence of a shift from most

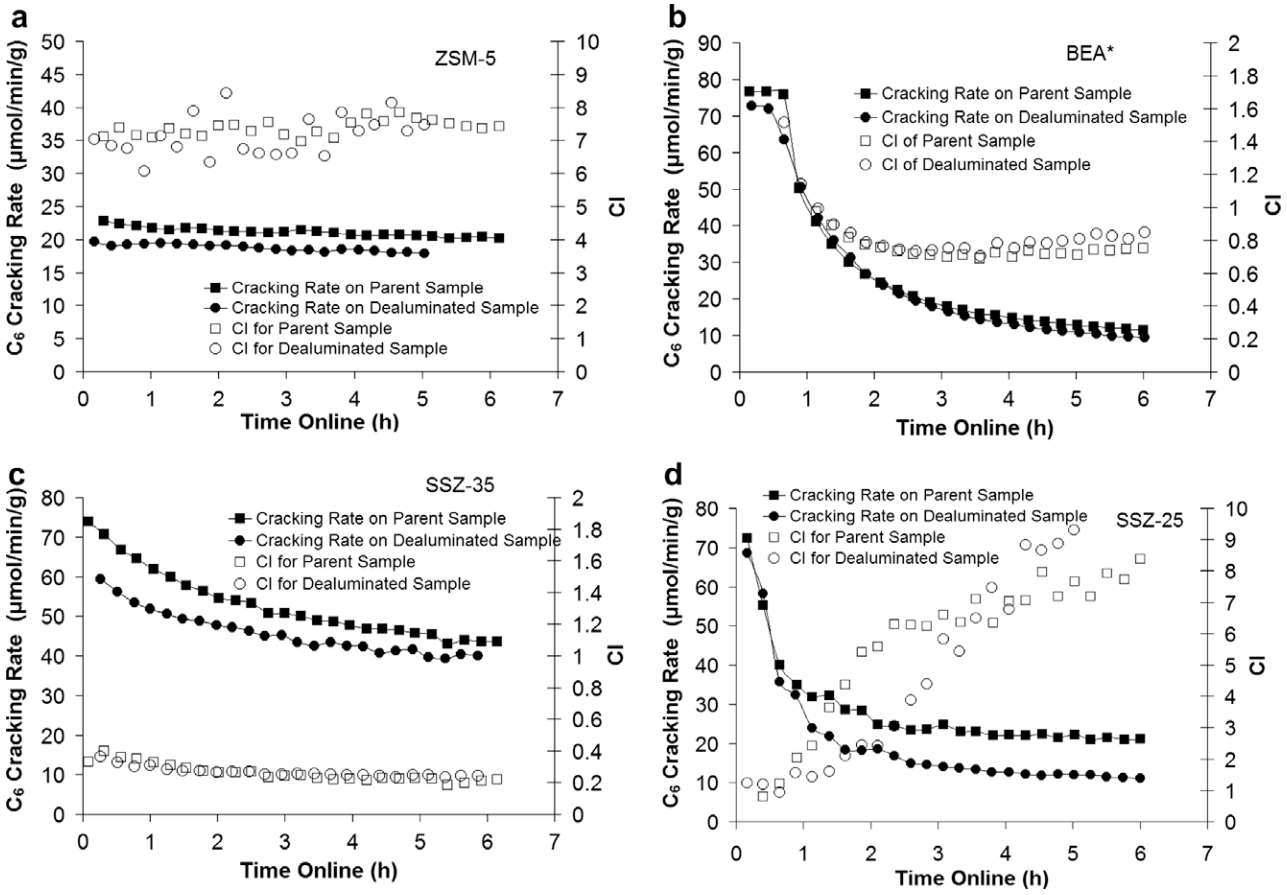

Fig. 3. CI test comparison between parent and dealuminated: (a) ZSM-5; (b) BEA; (c) SSZ-35 and (d) SSZ-25 at 315 °C. Parent samples have been calcined while dealuminated samples underwent the dealumination treatment then were calcined.

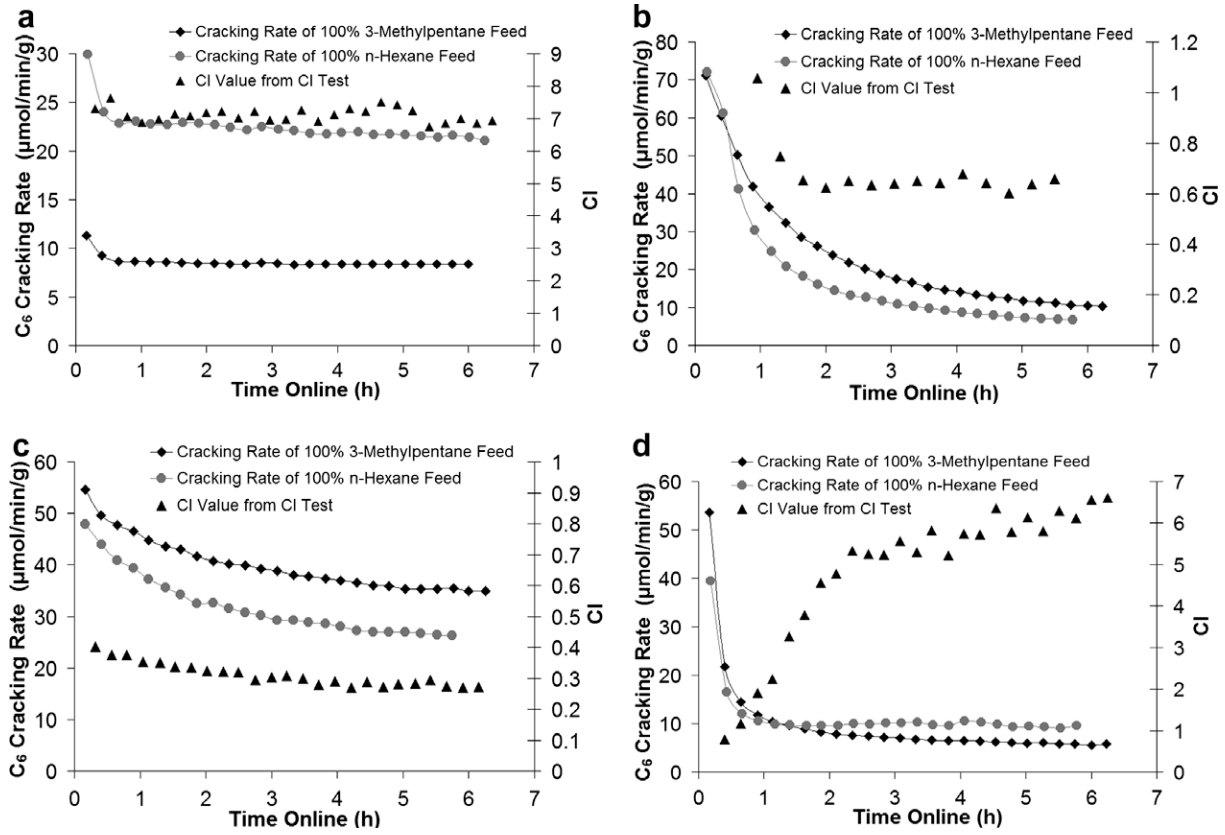

Fig. 4. Individual *n*-hexane and 3-methylpentane reactant cracking rates compared with CI values from the CI test on: (a) ZSM-5; (b) BEA; (c) SSZ-35 and (d) SSZ-25.

of the activity occurring in the large cages (initially giving a low CI value) to most of the activity occurring at later times from the sinusoidal channels (giving a high CI value). A similar change in the behavior of SSZ-25 is the shift in the *i*-C_4/*n*-C_4 product ratio over time. Zones and Harris detailed the link between *i*-C_4/*n*-C_4 product ratio and the CI value where higher CI values are associated with lower *i*-C_4/*n*-C_4 ratios, presumably due to less conversion of 3-methylpentane [2]. Additionally, Zones and Harris did not observe a change in the *i*-C_4/*n*-C_4 product ratio on ZSM-5 [2]. Here, for both the parent and the surface deactivated samples of SSZ-25, the *i*-C_4/*n*-C_4 ratio is around 5 at 15 min on stream and decays to 2.2 by 6 h on stream. For zeolites ZSM-5, BEA, and SSZ-35 the ratios are 1.1, 4.5, and 4, respectively, and remain relatively constant over 6 h on stream. With an inactive external surface, the change in *i*-C_4/*n*-C_4 ratio for SSZ-25 likely results from a shift in the primary location of the reaction from the cages in the structure to the more restricted sinusoidal channels. Since the pore sizes are similar between ZSM-5 and SSZ-25, the reaction data suggest the larger internal space of SSZ-25 is responsible for the CI value and its time dependence rather than external surface activity or pore size.

3.2. Effects of the presence of large cages

The effects of the presence of a large cage on the reactant accessibility to an active site and steric requirements for the reaction transition-states at that active center were investigated. Zones and Harris discussed this possibility for their observations of unusual results in the CI testing of large cage zeolites [2].

Transition-state selectivity has been invoked to explain the results of the CI value with some zeolite structures [17] and to describe the limited deactivation in hydrocarbon cracking with ZSM-5 [18]. Also, the deactivation in the reaction of *n*-heptane has been described to happen by coking which is limited to the large cages and not to the sinusoidal channels [16]. The results illustrated in Fig. 3 show that the activity of the ZSM-5 remains fairly constant over 6 h online while the other 10-ring structures and BEA show larger deactivation. Table 3 presents further data on the samples before and after the hydrocarbon reaction. ZSM-5 does accumulate mass during the reaction, but does so to a lesser degree than either of the other 10-ring structures when normalized to a per Al basis. All the caged structures continue to have mass accumulation at a larger rate than ZSM-5. Extrapolating the data from Table 3 to a constant conversion of 8.2 mmol C_6 cracked/mmol Al for all samples, the deposited mass in g deposited/mmol Al ranks the structures as ZSM-5 < SSZ-25 < SSZ-35 at 39.6, 42.1,and 46.6 g/mmol Al, respectively. SSZ-25 and SSZ-35 show a larger accumulation of mass than ZSM-5 that can be attributed to less steric constraints by the presence of the larger cages. Both SSZ-25 and SSZ-35 show micropore volume reductions greater than 80% from the volume of the parent materials while ZSM-5 remains relatively open with only a 15% reduction in micropore volume.

XPS and elemental analyses of the deactivated samples are listed in Table 3 and show % carbon increases for the samples from 1 h to 6 h on stream for the superficial area and bulk of the zeolites. ZSM-5 shows the smallest increase in carbon from 1 h to 6 h with an increase of 50% while SSZ-35 has a 60% increase and SSZ-25 increased at least 80%. By XPS analysis, the carbon increases in the superficial area of the zeolites are smaller for all samples and actually decrease for SSZ-35. The XPS analysis and elemental analysis showed the most similar change on ZSM-5. Comparing the increases measures by XPS and elemental analysis provides insight into the location of the deposition. Identical ratios would be observed for deposition only on the external surface while interior build up would result in a higher value from elemental analysis. The values obtained suggest larger internal deposition in SSZ-25

Table 3
Properties before and after CI testing on ZSM-5, SSZ-35 and SSZ-25.

Zeolite	Time online (h)	mmols C_6 cracked		Mass deposited mg of mass		Micropore vol. mL/g zeolite[b]	% Carbon increase from 1 h to 6 h online	
		g zeolite	mmol Al[a]	g zeolite	mmol Al[a]	(% reduced)[c]	Bulk[d] (%)	Surface[e] (%)
ZSM-5	1	5.5	8.2	26.7	39.6		50	30
	6	32	47	31.3	46.4	0.11 (15)		
SSZ-35	1	7.0	8.3	39.6	46.7		60	−30
	6	29	34	56.9	67.0	0.03 (80)		
SSZ-25	1	5.1	6.0	33.8	37.1		80	30
	6	14	15	52.7	57.8	0.02 (85)		

[a] mmols Al determined from elemental analysis, assumes all Al is in the framework.
[b] Determined by N_2 adsorption.
[c] % reduced as compared with calcined parent sample.
[d] Determined from elemental analysis.
[e] Determined from XPS measuring the near surface region.

and SSZ-35 than in ZSM-5. The ratios for SSZ-25 would most likely show an even larger difference if an earlier time point had been used because as can be seen in Fig. 3d a large portion of the deactivation attributed to the large cage has already occurred by the 1-h time point. These increases would also indicate that the larger space of the cages provides fewer limitations to the formation of the deactivating carbon species than in ZSM-5. These results would also be suggestive of less steric constraints for the transition-states giving rise to the CI value.

The cracking of pure feeds of *n*-hexane and 3-methylpentane provides further insights into the effects the presence of a large cage has on these reactions. Fig. 4 compares the cracking of pure feeds of *n*-hexane and 3-methylpentane with the CI value from the CI test over the time on stream for ZSM-5, BEA, SSZ-35, and SSZ-25. As expected from the CI test, ZSM-5 demonstrates a preference toward *n*-hexane cracking while BEA has a higher cracking rate of 3-methylpentane than *n*-hexane. (It is noted again that the branched isomer is expected to have a higher intrinsic activity than the linear isomer [1].) SSZ-35 has pore openings similar to ZSM-5 but the activity toward cracking *n*-hexane and 3-methylpentane is more like BEA. In addition to the cracking rates, the product distributions can provide useful information and the results from SSZ-35 are more similar to BEA than ZSM-5. Also, the i-C_4/n-C_4 ratio, when used as a measure of the product distribution between branched and linear products, is 4.8 for SSZ-35 while the ratio for BEA is 4.7 and ZSM-5 is only 1.8 for the cracking of 3-methylpentane. A similar result is seen for *n*-hexane cracking; however, the ratios are all lower. Hence, the cage in SSZ-35 results in a structure with a pore opening similar to ZSM-5 but cracking behavior similar to BEA. Also, with SSZ-35, the effect of the cage can be seen by comparison with ZSM-12, a 1-dimensional structure with 12-ring pore that is much smaller than BEA at 5.6 Å × 6.0 Å but larger than that of SSZ-35. ZSM-12 has a higher CI value, 2.1 as reported in the Zones and Harris study [2], than SSZ-35 and lower i-C_4/n-C_4 ratio, 2.5 [2], than SSZ-35 which has an i-C_4/n-C_4 ratio of 3.4 in the CI test. Thus the small increase in the pore opening size for SSZ-35 over ZSM-5 cannot account for the behavior of SSZ-35 being so similar to BEA.

The data presented in Fig. 4d for SSZ-25 show initially a very high activity with little difference in the activity for 3-methylpentane or *n*-hexane cracking. However, as the catalyst deactivates, a higher level of activity remains for *n*-hexane than 3-methylpentane. Since the pore size of SSZ-25 is smaller than that of ZSM-5, it is reasonable to consider that the sinusoidal channel system would have limited deactivation and favor *n*-hexane cracking like ZSM-5, and the large cages is where the majority of deactivation and mass accumulation occurs. The data presented in Fig. 4d support this interpretation. As with the CI values, the i-C_4/n-C_4 ratios for both 3-methylpentane and *n*-hexane cracking shift from behavior like BEA to that of ZSM-5 over time. For 3-methylpentane cracking, the initial i-C_4/n-C_4 ratio for SSZ-25 is 4.6 similar to BEA, and declines to almost 2 by 6 h online and is at that time closer to the ratio of ZSM-5.

3.3. Time dependent CI values

In addition to the lower than expected CI values from the structures with large cages, another feature of the CI value was the change in the value as a function of time online for SSZ-25. Zones and Harris [2] interpret this behavior as the expression of the difference in fouling rates for the two pore systems in the structure in a manner similar to that described by Guisnet and co-workers with *n*-heptane transformations over MCM-22 [16]. This type of behavior in the CI test with time online has also been observed with offretite [19]. Again, the results with offretite were interpreted to be due to the fouling of the larger 12-ring channels while slower deactivation occurred in the gmelinite cages. This interpretation was supported by experiments involving the poisoning of the solid by feeding pyridine and observing an increased initial CI value [19].

Typically, the CI value is reported at one time point between 20 and 40 min online. However, the CI test may also provide more evidence of zeolite structural features if the full dynamics of the reaction are explored. Mordenite has multiple pores systems and an increasing CI value with time online like offretite and SSZ-25. Studies by Weitkamp and co-workers [20] and Zones and Harris [2] demonstrated that both USY and BEA, respectively, have large-pore 3-dimensional structures that quickly foul, but maintain a similar CI value over 6 h online. Similarly in the same study by Weitkamp and co-workers, the 1-dimensional structure of ZSM-12 has large pores that show quick fouling but also maintains a fairly constant CI value over 6 h online [20]. The behavior of MOR (Si/Al ~6.5) can be interpreted in a manner similar to that of SSZ-25 and offretite where the large 12-ring channel fouls and the influence of the smaller side cages contributes to an increasing CI value.

Mordenite provides an opportunity to demonstrate that the time dependence of the CI value arises from the differences in the deactivation rates of the 8-ring side pockets and the 12-ring channels. Various works have shown that Na^+ cations preferentially exchange into the 8-ring side pockets in MOR [13,21,22]. Using the same ion-exchange conditions as described previously that achieved a complete exchange of the 8-ring side pockets [13], partial Na^+ exchanges were performed on a mordenite sample (Si/Al ~6.5) and then tested with the CI reactions. Fig. 5 shows data that compares the CI test for the calcined parent sample and the partial Na^+ exchanged sample of mordenite. In the partial Na^+ exchanged sample the CI value remains low at a level not unexpected

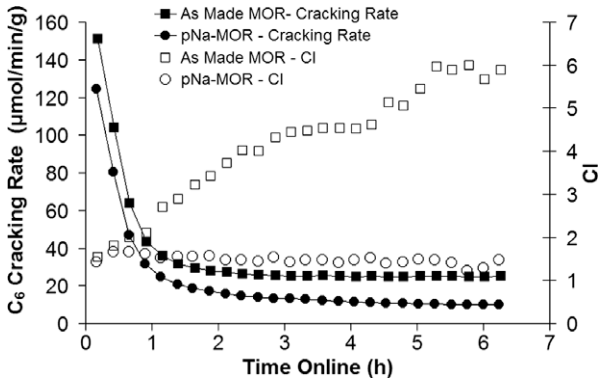

Fig. 5. Removal of the CI time dependence on MOR by partial Na^+-exchange. (pNa-MOR is the partially exchanged MOR using a 2.4 M $NaNO_3$ solution.)

for a large pore zeolite over the entire length of the run (no time dependence) and the cracking rate is less than half the cracking rate of the as-made sample. Lower levels of Na^+ exchange in the mordenite slowed the rate of increase in the CI value but did not eliminate the time dependence (data not shown). Partial Na^+ exchange on ZSM-5 did not affect the CI value while decreasing the activity (data not shown). The elimination of the time dependence of the CI value with mordenite by passivating the active sites in the 8-ring side pockets suggests that by extending the use of the CI test beyond a single point may provide insight into the presence of multiple pore features in a structure that have differing deactivation rates.

4. Conclusions

The presence of large cages in the structure of a zeolite can lower the CI value of that structure to values substantially lower than the expected value based on the size of the pore opening. This lowering of the CI value can make the classification of a structure as large, medium, or small pore more complicated. It is important to reiterate that the term "pore" can be confusing as there has been no clear delineation of its use in referring to either the portal, to the interior of the structure or to the entire passage space through the structure. The external surface of structures has very little influence on the CI testing as demonstrated on BEA, ZSM-5, SSZ-25, and SSZ-35, so only internal features of the structures need be considered. The CI test is not as predictive for the size of the structure portal when both *n*-hexane and 3-methylpentane can enter the structure, however, it can be indicative of the size of intracrystalline spaces, whether they are channels on the same size (as with ZSM-5 or larger openings on the same size as with BEA). When the cage sizes are significantly larger than the size of the portals, like what is found in SSZ25 and SSZ-35, then the CI test can provide results that are more dictated by the cage size rather than the portal size. Further, the CI test can provide more information beyond a one point value classification by use of the time dependence of the CI value to suggest the presence of multiple pore systems.

Acknowledgments

We would like to thank the Chevron Energy Technology Co. for financial support of this work and Kelly Harvey for assistance with the graphics and manuscript preparation.

References

[1] V.J. Frillette, W.O. Haag, R.M. Lago, J. Catal. 67 (1981) 218.
[2] S.I. Zones, T.V. Harris, Micropor. Mesopor. Mater. 31 (2000) 35.
[3] S.M. Csicsery, Zeolites 4 (1984) 202.
[4] P.A. Jacobs, J.A. Martens, Pure Appl. Chem. 58 (1986) 1329.
[5] P. Wagner, S.I. Zones, M.E. Davis, R.C. Medrud, Angew. Chem. Int. Ed. 38 (1999) 1269.
[6] F. Joensen, N. Blom, N.J. Tapp, E.G. Derouane, C. Fernandez, Stud. Surf. Sci. Catal. 49 (A) (1989) 1131.
[7] M.H. Kim, C.Y. Chen, M.E. Davis, ACS Symp. Ser. 517 (1993) 222.
[8] L-T Yuen, S.I. Zones, T.V. Harris, E.J. Gallegos, A. Auroux, Microporous Mater. 2 (1994) 105.
[9] J.A. Martens, M. Tielen, P.A. Jacobs, J. Weitkamp, Zeolites 4 (1984) 98.
[10] J. Weitkamp, S. Ernst, R. Kumar, Appl. Catal. 27 (1986) 207.
[11] F.R. Ribeiro, F. Alvarez, C. Henriques, F. Lemos, J.M. Lopes, M.F. Ribeiro, J. Mol. Catal. A: Chem. 96 (1995) 245.
[12] S.I. Zones, C.Y. Chen, A. Corma, M.T. Cheng, C.L. Kibby, I.Y. Chan, A.W. Burton, J. Catal. 250 (2007) 41.
[13] A. Bhan, A.D. Allian, G.J. Sunley, D.J. Law, E. Iglesia, J. Am. Chem. Soc. 129 (2007) 4919.
[14] S.I. Zones, S.-J. Hwang, M.E. Davis, Chem. – A Eur. J. 7 (2001) 1990.
[15] D. Breck, G. Skeels, US patent 4 503 023, 1985, to Union Carbide Corporation.
[16] P. Matias, J.M. Lopes, S. Laforge, P. Magnoux, M. Guisnet, F.R. Ribeiro, Appl. Catal. A: Gen. 351 (2008) 174.
[17] W.O. Haag, R.M. Lago, P.B. Weisz, Faraday Discuss. Chem. Soc. 72 (1981) 317.
[18] D.E. Walsh, L.D. Rollmann, J. Catal. 56 (1979) 195.
[19] F.R. Ribeiro, F. Lemos, G. Perot, M. Guisnet, in: R. Setton (Ed.), Chemical Reactions in Organic and Inorganic Systems, Reidel Pub. Co., 1986, p. 141.
[20] S. Ernst, R. Kumar, M. Neuber, J. Weitkamp, in: K.K. Unger, J. Rouquerol, K.S.W. Sing, H. Kral (Eds.), Studies in Surface Science and Catalysis, vol. 39, Elsevier, Amsterdam, 1988, p. 531.
[21] M.A. Makarova, A.E. Wilson, B.J. van Liemt, C. Mesters, A.W. de Winter, C.J. Williams, J. Catal. 172 (1997) 170.
[22] V.A. Veefkind, M.L. Smidt, J.A. Lercher, Appl. Catal. A 194 (2000) 319.